JCTC Journal of Chemical Theory and Computation

Article

pubs.acs.org/JCTC

Scalable Anisotropic Shape and Electrostatic Models for Biological Bromine Halogen Bonds

Megan Carter,[†] Anthony K. Rappé,[‡] and P. Shing Ho*,[†]

[†]Department of Biochemistry and Molecular Biology and [‡]Department of Chemistry, Colorado State University, Fort Collins, Colorado 80523, United States

ABSTRACT: Halogens are important substituents of many drugs and secondary metabolites, but the structural and thermodynamic properties of their interactions are not properly treated by current molecular modeling and docking methods that assign simple isotropic point charges to atoms. Halogen bonds, for example, are becoming widely recognized as important for conferring specificity in protein−ligand complexes but, to this point, are most accurately described quantum mechanically. Thus, there is a need to develop methods to both accurately and efficiently model the energies and geometries of halogen interactions in biomolecular complexes. We present here a set of potential energy functions that, based on fundamental physical properties of halogens, properly model the anisotropic structure−energy relationships observed for halogen interactions from crystallographic and calorimetric data, and from *ab initio* calculations for bromine halogen bonds in a biological context. These energy functions indicate that electrostatics alone cannot account for the very short-range distances of bromine halogen bonds but require a flattening of the effective van der Waals radius that can be modeled through an angular dependence of the steric repulsion term of the standard Lennard-Jones type potential. This same function that describes the aspherical shape of the bromine is subsequently applied to model the charge distribution across the surface of the halogen, resulting in a force field that uniquely treats both the shape and electrostatic charge parameters of halogens anisotropically. Finally, the electrostatic potential was shown to have a distance dependence that is consistent with a charge-dipole rather than a simple Coulombic type interaction. The resulting force field for biological halogen bonds (*ff*BXB) is shown to accurately model the geometry−energy relationships of bromine interactions to both anionic and neutral oxygen acceptors and is shown to be tunable by simply scaling the electrostatic component to account for effects of varying electron-withdrawing substituents (as reflected in their Hammett constants) on the degree of polarization of the bromine. This approach has broad applications to modeling the structure−energy relationships of halogen interactions, including the rational design of inhibitors against therapeutic targets.

INTRODUCTION

Accurate methods to model noncovalent molecular interactions are crucial to "bottom-up" strategies in biomolecular engineering. Current molecular mechanics (MM) force fields are powerful tools for modeling biomolecular systems and have, for example, been successful in accurately predicting affinities of ligands in various protein complexes.[1] Halogens are typically considered to be hydrophobic substituents that are electron-rich and, as a consequence, should repel electronegative atoms; however, halogens as covalent substituents in organic and biomolecular molecules are now recognized as displaying simultaneously electronegative and electropositive potentials, allowing them to serve both as hydrogen bond (H-bond) acceptors[2] and as halogen bond (X-bond) donors.[3] Their electrostatic properties, therefore, are highly directional and should be treated as such. In this study, we have derived a set of potential energy functions that describe the aspherical shape and anisotropic distribution of electrostatic potentials of bromines, thereby providing a framework for the structure−energy relationships that can accurately model the ability of halogens to simultaneously participate in X- and H-bonding interactions.

Halogen bonds, formerly called "charge transfer bonds",[4] have seen a resurgence of interest as a tool to engineer new molecular materials,[5] including, in medicinal and biophysical chemistry, the design of new protein inhibitors[6] and for directing DNA conformations.[7] X-bonds are closely related to the better-known hydrogen bonds (Figure 1a and b)[8] in that both have donor−acceptor distances that can be significantly shorter than the sum of their respective van der Waals radii ($\sum r_{vdW}$) and share a common set of acceptors (we adopt definitions that are analogous to that of H-bonds, where the X-bond donor donates a positive charge from polarization of the halogen and the acceptor is an electron-rich atom or group involved that pairs with the donor[3a,5]).

The X-bond "donor" is an electropositive cap resulting from polarization of the halogen (X) along the C−X σ-bond (Figure 1c). The "σ-hole" model[2a,9] provides a simple, primarily electrostatic description of this phenomenon:[10] in this model, the valence electron in the outer shell p_z orbital participates in the formation of the covalent σ-bond, leaving the orbital depopulated and, thus, exposing the nuclear charge that is the electropositive crown opposite the covalent bond. The degree to which the orbital is polarized follows the series I > Br > Cl > F, which defines the order of stabilizing energies of the X-bond.[11] The p_x and p_y orbitals, however, remain fully occupied, thereby providing an electronegative annulus around the halogen that serves as a potential H-bond acceptor perpendicular to the σ-bond. Thus, the polarized halogens are

Received: March 7, 2012
Published: May 29, 2012

   dx.doi.org/10.1021/ct3001969 | *J. Chem. Theory Comput.* 2012, 8, 2461−2473

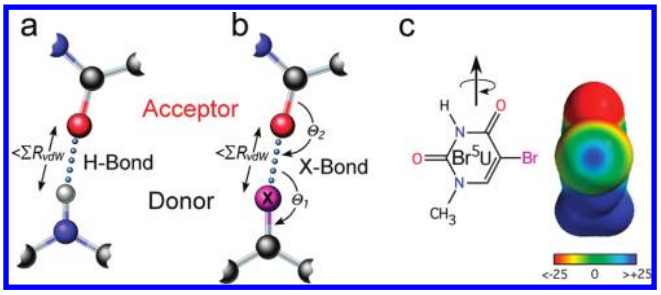

Figure 1. Hydrogen and halogen bonds. (a) The hydrogen bond (H-bond) is a noncovalent interaction in which the approach of the hydrogen donor to the acceptor atom (red) is closer than the sum of their van der Waals radius ($\sum R_{vdW}$). (b) Similarly, the halogen bond (X-bond) brings the halogen donor (magenta) closer to the acceptor (red) than their $\sum R_{vdW}$. As a highly directional interaction, the X-bond is also defined by the angle of approach of the acceptor to the donor (Θ_1) and the donor to the acceptor (Θ_2). (c) The bromine substituent of a 5-bromouracil (Br^5U) base is modeled to show the positive crown resulting from polarization along the C−Br bond. Electrostatic potentials (from −25 kcal/mol to +25 kcal/mol) were estimated from DFT calculations.[3a]

amphoteric, serving both as X-bond donors in one direction and classical H-bond acceptors in the perpendicular direction.[2] There is an understanding, however, that X-bonding is not solely an electrostatic effect but that dispersion and, to a lesser extent, charge transfer also contribute at least to the energetics of the interaction.

X-bond acceptors in biological systems include both charged and uncharged oxygens, amino and imino nitrogens, sulfurs, and aromatic rings.[3a,12] Their energies of interaction depend strongly on the geometries relating the donor and the acceptor.[3a,12a] X-bonds are highly directional,[11] with geometries defined by the angular approach of the acceptor toward the halogen (Θ_1) and of the halogen to the acceptor (Θ_2; Figure 1): Θ_1 is generally in the direction of halogen polarization,[3a,8,11,13] while Θ_2 aligns with the nonbonding or π electrons of the acceptor.[14]

The contribution of polarization to halogen interactions[14,15] is most accurately modeled through quantum mechanical (QM) and semiempirical QM methods[16] but is poorly treated by MM algorithms that treat atoms classically as single point charges.[17] QM calculations applying density functional theory (DFT) on the ultrahigh resolution aldose reductase/inhibitor structure[18] had identified an X-bond that accounts for the high specificity of the inhibitor for this enzyme, while the semiempirical PM6-DH2X method has been shown to accurately model both the geometries and binding energies of several kinase inhibitors.[17] Finally, hybrid QM/MM approaches[19] have seen some success in modeling X-bonds in protein−ligand complexes.[13] However, QM calculations on biomolecules remain very time intensive and are subject to cumulative errors in atomic coordinates. There is, therefore, a great need for an accurate molecular mechanics force field for biological X-bonds that is consistent with and, therefore, can be incorporated into current MM algorithms to facilitate our ability to exploit halogens as design elements in engineering biomolecular interactions.

Recently, there have been attempts to model the positive crown of halogens and their associated X-bonds using a positive extra-point (PEP) approach, where an additional partial positive point charge is added, displaced at some distance from the atomic center, while maintaining the overall negative charge of the halogen. The work of Ibrahim[20] on small molecular systems as well as protein−inhibitor complexes demonstrates that such an approach can be useful in modeling X-bonds in multiple systems. From molecular dynamics studies applying the AMBER MM force field, the PEP method was capable of reproducing the X-bond lengths (to within 0.1 to 0.29 Å, with an RMSD of 0.2 Å) and energies (within 0.1 to 0.37 kcal/mol, RMSD 0.27 kcal/mol) from MP2 calculations of bromobenzene donors to various acceptors. In addition, the PEP approach was capable of calculating inhibitor binding energies to CK2 kinases that correlated well (R values of 0.92 to 0.96) with the experimental values, with acceptors approaching the halogens at near linear angles. The absolute energies, however, were significantly more negative (by ∼20 kcal/mol) than the experimental values, and the calculated X-bond lengths were significantly longer than those seen in the X-ray structures (this could be attributed to waters that were crystallographically observed in the active site but absent from the AMBER models). Thus, the field of developing MM models for X-bonds remains open to improvements and new approaches.

In the current studies, we derive a set of simple directional potential energy functions to model the shape and electrostatic properties of halogens, which, together, constitute a set of potential energy functions for a force field for biological halogen bonds (*ff*BXB). This differs from attempts at modeling X-bonds using a purely electrostatic PEP approach[21] in that the *ff*BXB attempts to also model both the repulsive steric and attractive dispersion contributions to the physicochemical properties of halogen interactions—although the σ-hole model for X-bonds does not explicitly consider steric and dispersion terms, we show that the size and shape of the halogen is aspherical, which we interpret to be attributable to the depopulation of the atomic p_z orbital, a hallmark of the σ-hole model. The *ff*BXB functions are parametrized against the AMBER force field[19a] and applied to the structure−energy relationships of X-bonds derived from a four-stranded DNA junction system studied in crystals[7] and in solution.[22] We have developed four-stranded DNA junctions as a unique model system to assay the energies of X-bonds in a biological context, where a halogen interaction competes against a classic H-bond in stabilizing the complex (Figure 2). The energies of two geometries (the longer Br1J and shorter Br2J X-bonds) have been characterized for bromine X-bonds ($Br\cdots O^-$) in this system and have shown that the steric and hydrophobic properties of the bromine essentially compensate for the stabilizing potential of the competing H-bond; thus, the experimental energies can be applied directly as an empirical test for a set of QM calculations as well as the *ff*BXB functions derived from them.

We then apply the *ff*BXB to map the geometry−energy relationships of X-bonds with formally neutral oxygens (the primary interactions seen in complexes of halogenated ligands with the peptide backbone of protein[3a,12c,14]), to predict the geometries of potential H-bonds to bromines (demonstrating the ability of the potential energy functions to model the amphoteric properties of halogens), and to develop parameters for PEP models that approximate and, thus, can be compared and contrasted with the structure−energy relationships of the *ff*BXB. The quality of each model is measured by their correlation with QM and experimental energies for the X-bonds in the DNA junction system as well as QM energies for a

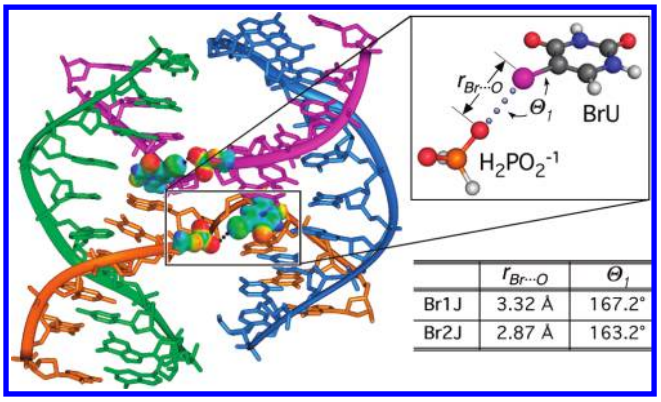

Figure 2. Model for bromine X-bond in DNA junction. A four-stranded DNA junction stabilized by an X-bond from the bromouracil base at the nucleotide N7 position to the phosphate backbone at N6 of the crossing strand of the junction. The inset shows the bromouracil (BrU) to hypophosphite ($H_2PO_2^-$) pair used to model the X-bond interaction within the DNA, along with the distance (r) and angle (Θ_1) definitions for the geometry of the interaction between the bromine X-bond donor and the oxygen acceptor. Two specific geometries are observed for the X-bond in the DNA junction,[7] with the longer Br1J being less stable than the shorter Br2J form.

bromobenzene···acetone pair, which serves as a model for X-bonds in protein systems.

THEORY AND METHODS

The primary goal of the current study is to derive a set of potential energy functions that accurately describes the short-range and angular dependent properties of halogen bonding interactions in the context of a biological system. The biological system we chose to model is that of a four-stranded DNA junction (Figure 2), which has been shown to be stabilized by and whose conformation can be controlled by X-bonding.[7,22] For this set of studies, we focus on bromine, which has been the most extensively studied in the DNA system in terms of the experimentally derived structure–energy relationships, and for which the steric and hydrophobicity contributions to the interaction largely balance the energy of the competing H-bond.[22] In this system,[7] the energy is directly correlated with specific distances and geometries of the interaction in a crystal, with the crystal-state energies seen to correlate well with those in solution.[22]

Our initial attempt to model the structure–energy relationship of X-bonds started by determining whether a standard set of potentials applying single-point charges in a Coulombic function and van der Waals functions could describe the geometries seen in the DNA junction system. We found that a stabilizing potential could be calculated for an X-bond with the acceptor approaching the bromine in a linear orientation to the σ-bond; however, in order to allow an oxygen to approach the bromine to within 2.9 Å (near the optimum distance for the interaction), the halogen had to be assigned an unusually large positive charge ($+2e$), or the potential energy well for the van der Waals interaction of the Br···O pair needed to be set at <10% of the standard values (data not shown). In either case, the energies from this simplistic model did not fit well with the observed experimental results, showing a 3.3 Å X-bond to be ~4 kcal/mol more favorable than the shorter 2.9 Å interaction. We, therefore, need to treat the basic physicochemical properties of halogens as substitutents in molecular systems in a different way.

To develop a more accurate model for halogens, we started with a set of very basic questions: What is the physical shape of a bromine substituent in a covalent molecule? What determines this shape, and can the shape be modeled empirically? We then determine whether the same principles that dictate the shape can be applied to model the anisotropic electrostatic properties of the halogen. The resulting potential energy functions that describe the shape and electrostatic properties are then parametrized against QM calculations on a minimum molecular model for the enthalpic components of the interaction in the experimental DNA system and, finally, extrapolated to broader classes of interactions of halogens in other biological contexts.

Effective Shape of Bromine. The effective shape of an atom in a molecule can be described by the two competing terms of the van der Waals (vdW) interaction (E_{vdW}): the attractive dispersive London forces acting at long distances are opposed by the steric repulsive forces at short distances. We

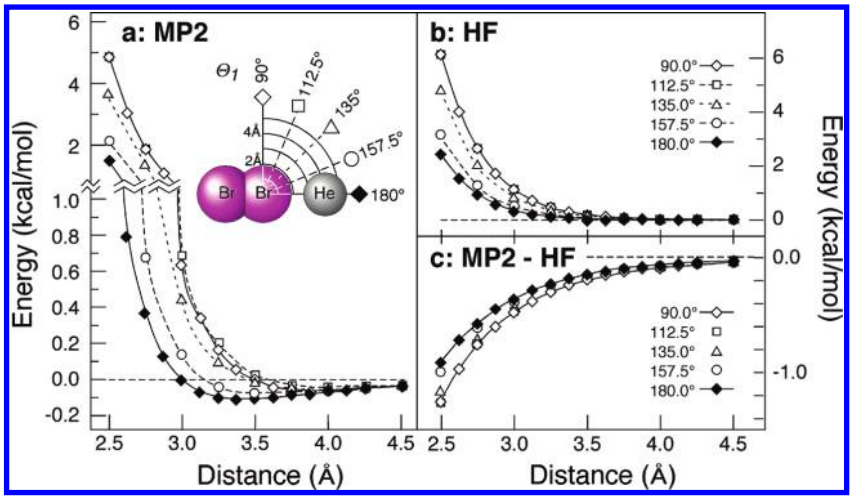

Figure 3. Quantum chemical calculations (applying augmented cc-pVTZ basis) mapping distance–angle relationship of He interacting with Br_2. (a) (MP2) Calculations applied to He···Br distances from 2.5 to 5.0 Å (data to 4.5 Å shown), and He···Br–Br angles (Θ_1) from 90° to 180°, in 22.5° increments. (b) Hartree–Fock (HF) calculations on the same system as a. (c) Difference between the MP2 and HF calculated energies. Curves connecting each point have been added to show trends and have no theoretical basis in this figure.

dx.doi.org/10.1021/ct3001969 | J. Chem. Theory Comput. 2012, 8, 2461–2473

mapped the effective atomic radius of a bromine starting with a simple Br_2···He interaction pair, placing the He atom at distance intervals from 2.5 to 5 Å for angles from 90° to 180° (in 22.5° steps). Since He is a small, nonpolarizable atom, high level *ab initio* calculations on this model complex allow us to focus on the distance and angle dependence of the competing attractive and repulsive[22] components, similar to previous approaches used to map the shape of chlorine.[23] Second-order Møller−Plesset (MP2) calculations[24] show the total E_{vdW} for the Br···He interaction to be strongly dependent on the angle of approach of the He atom relative to the Br−Br covalent bond, Θ_1 (Figure 3a). These results indicate that the shape of bromine is aspherical, with the effective van der Waals radius (R_{vdW}) being ∼0.5 Å shorter when approaching along as opposed to perpendicular to the Br−Br bond.

To establish the root of the aspherical shape of the bromine, a Hartree−Fock (HF) calculation was applied to this Br_2···He model to probe the repulsion energies in the absence of any dispersive interactions. This analysis showed that the repulsive term is also highly dependent on Θ_1 (Figure 3b). At the standard van der Waals distance ($\sum R_{vdW}$ = 3.25 Å), there is an ∼0.33 kcal/mol difference between the linear (Θ_1 = 180°) and the perpendicular (Θ_1 = 90°) approaches. Similarly, the distance at which the repulsion energy is 1 kcal/mol extends from ∼2.7 Å for the linear to ∼3.0 Å for the perpendicular approach. By subtracting the HF energies from the MP2 calculated energies, we can estimate the contribution of dispersion to the overall E_{vdW} (Figure 3c). The dispersion component is seen to be relatively independent of Θ_1, with a difference of <0.4 kcal/mol between the linear and perpendicular approach at a 2.5 Å distance. Thus, the angle dependence of the interacting atoms derives primarily from the repulsion term, allowing us to treat the dispersive component as essentially isotropic in terms of the effective R_{vdW} for the bromine.

In order to relate these results to the effective shape in terms of the van der Waals radius (R_{vdW}) of the bromine atom, we fit the overall MP2 calculated E_{vdW} to a modified Lennard-Jones type potential energy function (V_{LJ}) in which the repulsive ($1/r^{12}$) component is treated as a function of the Θ_1 angle, while the dispersion ($-1/r^6$) component is angle independent (eq 1). For the angle dependent term, we define an effective average van der Waals radius for the bromine ($\langle R_{vdW(Br)} \rangle$) that is applied to both components, but with a $\Delta R \cos[\nu\alpha]$ added only to the repulsive component, where ΔR is a perturbation to the $\langle R_{vdW(Br)} \rangle$, ν is the period of the cosine function for the Θ_1 dependence, and $\alpha = 180° - \Theta_1$.

$$V_{LJ} = 4\varepsilon\left[\left(\frac{R_{vdW(He)} + \langle R_{vdW(Br)}\rangle - \Delta R\cos(\nu\alpha)}{r}\right)^{12} - \left(\frac{R_{vdW(He)} + \langle R_{vdW(Br)}\rangle}{r}\right)^{6}\right] \quad (1)$$

A nonlinear least-squares fit of the V_{LJ} function in eq 1 to the distance−angle dependence of E_{vdW} from the MP2 calculations results in a set of values for $\langle R_{vdW(Br)} \rangle$, ΔR, and ν that describes the overall shape of the bromine in Br_2. The resulting $\langle R_{vdW(Br)} \rangle$ = 1.816 Å is only slightly shorter than the accepted isotropic 1.85 Å value,[25] while the ΔR of 0.157 Å indicates that there is a significant flattening of the Br atom along the σ-bond (Θ_1 = 180°) and bulging approximately perpendicular to the bond. The minimum and maximum effective $R_{vdW(Br)}$ range from 1.66 Å to 1.97 Å, equivalent to a ∼16% (0.314 Å) difference between the smallest and largest effective radius (Figure 4). A similar polar flattening of 0.37 Å was reported from an analysis of the crystal structures of Br_2 complexes.[26] The value of ν = 2.53 indicates that the bulge is at Θ_1 = 108.9° rather than at the 90° expected for the ideal orientation of the p_x and p_y orbitals (ideally, ν = 2.0), relative to the covalent Br−Br bond, suggesting that these orbitals are canted ∼19° from perpendicular and toward the depopulated p_z orbital. This nonperpendicular bulge is consistent with recent calculations on the multipolar electron densities showing the maximum charge concentration for bromine from 95° to 110° relative to the C−Br bond (personal communication, Prof. E. Espinosa, Université de Nancy, France).

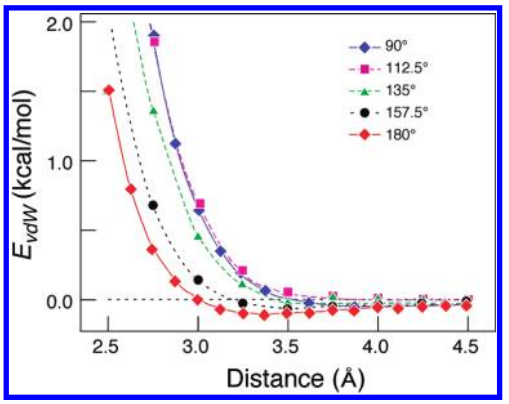

Figure 4. QM calculated van der Waals energy (E_{vdW}) fitted as a directional Lennard-Jones potential (eq 1). The fitted parameters result in an overall correlation coefficient of 0.987, with a standard deviation between the MP2 calculated and fitted curves of 0.155 for $E_{vdW} \leq$ 1.0 kcal/mol.

Effective Partial Charge and Electrostatic Potential Function for Bromine. The basic premise of the σ-hole model for halogen bonding is that the p_z orbital of covalently bonded halogen is depopulated when forming the σ-bond. Consequently, an electropositive cap is created from polarization of the electrostatic potential along this bond, and it is this cap that interacts with electron-rich acceptors, such as negative and neutrally charged oxygens, sulfurs, and nitrogens. Overall, bromines are considered to be slightly negatively charged but can carry a partial positive charge when bound to a strongly electron withdrawing atom or group[27] (as in BrCl). Thus, the aspherical shape of the bromine described above would suggest an anisotropic charge distribution across the atomic surface of bromine, with the effective charge being most positive for a linear approach toward the σ-bonded Br and most negative for an approximate perpendicular approach. This is indeed what has been observed in QM calculations of charge distributions across various halogens.[2b,10]

A simple model to describe such an anisotropic charge distribution would be to apply the same cosine function that was used to model the aspherical shape of the bromine to define the effective partial charge of the bromine (Z_{Br}) as a function of the approach angle ($\alpha = 180° - \Theta_1$; eq 2).

$$Z_{Br} = A\cos(\nu\alpha) + B \quad (2)$$

In this form, the cosine function is identical to that in eq 1, with the parameter A introduced to scale the amplitude of the cosine

function and B to define the baseline for where the positive and negative charges cross.

The period (ν) of the function and the ratio of A/B were determined by applying eq 2 to the previously reported electrostatic potential distribution for a bromine of bromobenzene[2b] (Figure 5). The fitted period of the cosine function

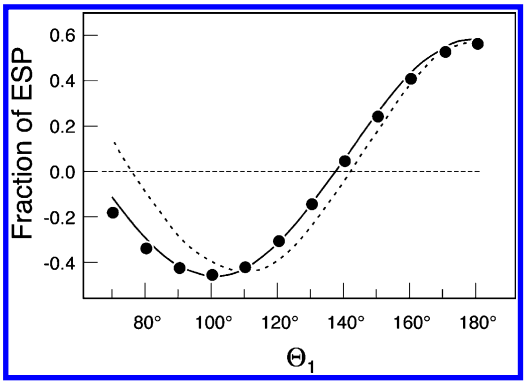

Figure 5. Electrostatic potential of bromine as a function of Θ_1. The fraction of the electrostatic potential (ESP, solid circles) calculated for the bromine in a bromobenzene model calculated using MP2/aug-cc-pVDZ[2b] and scaled to the difference in the maximum and minimum ESP values. Fraction of partial charge of the bromine fitted to eq 2 with $\nu = 2.231 \pm 0.008$, and a ratio of $B/A = 0.124 \pm 0.005$ (solid curve). The dotted curve represents the fraction partial charge predicted for $\nu = 2.535$ associated with the shape analysis (Figure 4).

places the most negative partial charge at ~99.3°, or nearly perpendicular to the covalent bond, indicating that the orientations of the p_x and p_y orbitals are dependent on the context of the bromine as a substituent—the phenyl group is less electronegative than a bromine substitutent, and therefore, the p_z-orbital electrons are expected to be less depopulated in bromobenzene than for Br_2.

The overall charge of the bromine in this anisotropic model was estimated by considering the charge at each angle α (from 0° to 90° in 5° increments) as defined by eq 2 and scaling that to the area associated with the surface in the increment from α_1 to α_2 according to eq 3:

$$SA(\alpha_1 \rightarrow \alpha_2) = 2\pi \int_{\alpha_1}^{\alpha_2} (\langle R_{o(\mathrm{Br})} \rangle - \Delta R \cos(\nu\alpha) \sin\alpha \, d\alpha$$
$$= \pi(2\langle R_{o(\mathrm{Br})} \rangle \cos\alpha - \Delta R(\sin[(1+\nu)\alpha] + \sin[(1-\nu)\alpha])|_{\alpha_1}^{\alpha_2} \quad (3)$$

The resulting overall normalized partial charge of the bromine is estimated to be $Z_{Br} = -0.14e$, similar to results from MP2 calculations. The bromine is seen to be effectively positively charged for $\Theta_1 \geq 130°$, allowing it to serve as an X-bond donor in this range, and negative for $\Theta_1 \leq 130°$, serving as an H-bond acceptor.

The effective Z_{Br} can be placed in the context of a general distance (r) dependent electrostatic potential energy function (V_{Elec}, analogous to a Coulombic potential) when paired with an acceptor with charge Z_A, as in eq 4 (where D is the dielectric constant and e is the charge of a proton). In this general form, we make no assumptions concerning the exponential power term n for the dependence of the potential energy on $1/r^n$.

$$V_{\mathrm{Elec}} = \frac{Z_{\mathrm{Br}} Z_{\mathrm{A}} e^2}{D r^n} \quad (4)$$

RESULTS

Potential Energy Function for Bromine. The overall potential energy for the nonbonding interactions between a bromine donor and an acceptor atom (V_{Br}) is given as the sum of the vdW and electrostatic potentials. In order to compare this potential energy function to the PEP approach, we have rewritten the equations to be consistent with the AMBER force field (eq 5, where $\varepsilon = (\varepsilon_1\varepsilon_2)^{1/2}$, with ε_1 and ε_2 being the energy contributions and R_o being the effective atomic radii of each of the two interacting atoms potential energy minimum) and will parametrize the V_{Br} function against the AMBER ff99[19a] force field, because of its broad use in simulating macromolecular structures and its adaptability to several molecular mechanics modeling programs[28] (including CHARMM[29] and GROMACS[30]).

$$V_{\mathrm{Br}} = V_{\mathrm{LJ}} + V_{\mathrm{Elec}} = \varepsilon\left[\left(\frac{\sum R_o}{r}\right)^{12} - \left(\frac{2\sum R_o}{r}\right)^{6}\right] + \frac{Z_{\mathrm{Br}} Z_{\mathrm{A}} e^2}{D r^n} \quad (5)$$

For the bromine, which follows the σ-hole model, the total potential function is dependent on $\alpha = 180° - \Theta_1$ according to eq 6, where $\langle R_{o(\mathrm{Br})} \rangle$ is now the average radius of the bromine at the energy minimum.

$$V_{\mathrm{Br}} = \varepsilon\left[\left(\frac{R_{o(\mathrm{A})} + \langle R_{o(\mathrm{Br})} \rangle - \Delta R \cos\nu\alpha}{r}\right)^{12} - \left(\frac{2(R_{o(\mathrm{A})} + \langle R_{o(\mathrm{Br})} \rangle)}{r}\right)^{6}\right] + \frac{[A\cos(\nu\alpha) + B] Z_A e^2}{D r^n} \quad (6)$$

Parameters for Bromine Potential Energy Functions. In order to parametrize V_{Br} in eq 6, we start by defining a biomolecular system for which there are good estimates for the distance−angle dependence of the nonbonded interaction energy. We then use the structure−energy relationship for this X-bonded system calculated by QM methods to determine values for the parameters in eq 6. Finally, crystallographic and solution-state studies on the structure and energies of the interactions in this system are used to validate both the QM calculations and the parametrized potential energy equation. For this study, we selected the bromouracil−phosphate ($BrU\cdots PO_4^-$) interaction from the competition assay in a four-way DNA junction[7,22] as the biomolecular system—the energies of interaction in this system have been experimentally determined for two unique X-bond geometries (Br1J and Br2J, Figure 2). The overall strategy is to (*i*) define a minimum model system for the relevant X-bond interaction in the DNA, (*ii*) calculate MP2 energies for the interaction at various distances and angles, (*iii*) derive parameters for the potential energy functions in eq 6 to be consistent with the AMBER ff99[19a] force field for all nonhalogen interactions to create a force field for the bromine halogen bond, and (*iv*) compare the calculated energies to the MP2 calculated energies and to those for the two experimental geometries.

The system for QM calculations was reduced from the complete DNA junction (with over 600 non-hydrogen atoms) to a simple bimolecular pair of an isolated BrU base interacting

dx.doi.org/10.1021/ct3001969 | J. Chem. Theory Comput. 2012, 8, 2461−2473

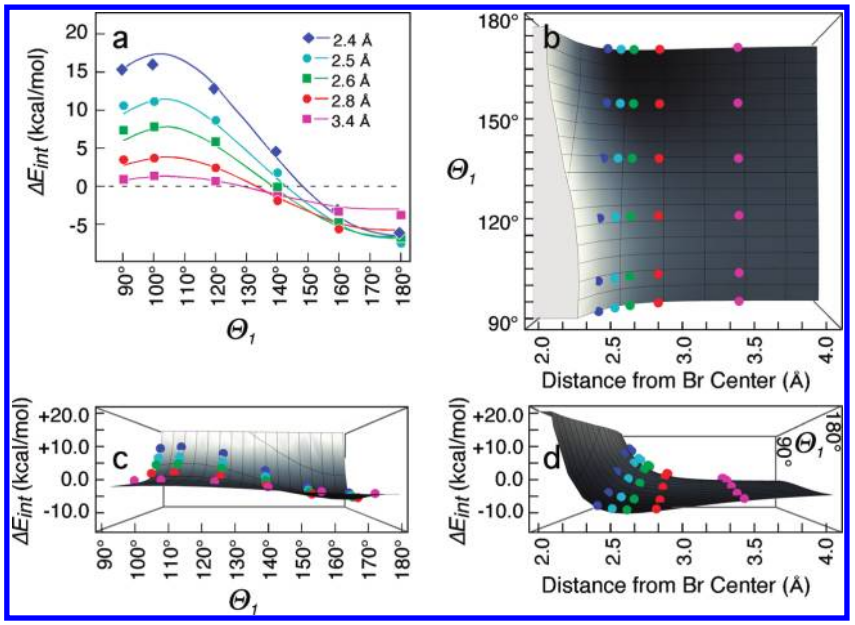

Figure 6. Energies of the BrU···$H_2PO_2^-$ interaction as a function of the angle and distance. (a) Results from MP2/6-31G(d) quantum calculations for the interacting system are shown as closed symbols. Curves are calculated energies from the V_{Br} function (eq 6) for the angles and distances associated with the QM calculations. The resulting QM calculated energies are mapped onto an energy landscape from the V_{Br} function (eq 6) of the *ff*BXB model (b, viewed onto the angle-distance surface; c, into the energy-angle plane; d, into the energy distance plane).

Table 1. Parameters for the Angle-Dependent *ff*BXB Functions Describing the Anisotropic Shape and Electrostatic Potential Energy Functions for the Bromine of BrU (eq 6)[a]

shape parameters			electrostatic parameters			angle
$\langle R_{o(Br)} \rangle$	ΔR (Å)	ε_{Br}(kcal/mol)	A	B	n	ν
2.04 Å	0.060 ± 0.022	0.019 ± 0.002	2.84 ± 0.82	1.53 ± 0.45	2.29 ± 0.29	2.31 ± 0.02

[a]Errors are indicated for fitted parameters.

with a hypophosphite ($H_2PO_2^-$) anion (Figure 2). The $H_2PO_2^-$ model for the phosphate group in the DNA system was selected because the MP2 calculated partial charge of the oxygens closely mirrored the partial charges in the AMBER force field (approximately $-0.85e$). Although the system is now reduced to only 17 atoms, it is still too computationally costly to perform the highest-level quantum calculations for the number of distances and angles required to fully define a geometry–energy relationship. Thus, we applied MP2 calculations using the 6-31G(d) basis set, with cyclohexane as the solvent ($D = 2$) and a counterpoise correction for the basis set superposition error,[31] on the model with the closest bromine to oxygen approach of the BrU·$H_2PO_2^-$ pair varied from 2.4 to 3.4 Å and for Θ_1 angles from 90° to 180°. We note that the relative energies calculated for the two defined geometries of Br1J and Br2J were very similar among various basis sets and different values for D, even though the absolute energies differ.

The resulting MP2 calculations show an angle dependence for the energies at each distance which is sinusoidal with a crossover from positive to negative energies at $\Theta_1 \approx 140°$ (Figure 6a), mirroring the relationships for the electrostatic potential energies (Figure 5). Indeed, at a distance $r = 2.8$ Å, the shape and crossover from positive to negative energies is nearly an exact reflection of the angle dependence for the partial charge of the bromine, consistent with a strong contribution of electrostatics on the interaction, as expressed by the σ-hole model.

We used the MP2 calculated energy–geometry relationship to determine the parameters for V_{Br}, as defined by eq 6. For this process, we first applied the AMBER type Lennard-Jones and electrostatic potentials to calculate the atom-to-atom interaction energies between the atoms in the BrU and $H_2PO_2^-$ molecular pair, excluding those involving the bromine, for each geometry of the model. Since we do not include explicit solvent in the model, a distance dependent dielectric[32] of the form $4r$ was applied to all of the electrostatic potential energy calculations. These non-Br energies ($E_{non\text{-}Br}$) were subtracted from the MP2 calculated energies (E_{MP2}) to yield a residual that describes explicitly the energy of the bromine interacting with the atoms of the $H_2PO_2^-$ component ($E_{Br} = E_{MP2} - E_{non\text{-}Br}$). This E_{Br} was subsequently used to determine the parameters for the V_{Br} potential function in eq 6.

The function for V_{Br} includes seven unique parameters: $\langle R_{vdW(Br)} \rangle$ and ΔR to describe the average van der Waals radius and perturbation to that radius and ε_{Br} to define the bromine contribution to the minimum van der Waals energy; A and B for the partial charge and n for the exponential dependence of the electrostatic potential on r; and ν for the period of the cosine function that describes the aspherical shape and charge distribution for the bromine (Table 1), which will be fitted against 30 MP2 calculated energy–geometry relationships. We considered the $\langle R_{vdW(Br)} \rangle$ from the shape analysis to be very robust and, therefore, converted this to an $\langle R_{o(Br)} \rangle = 2.04$ (recalling that the two radii are related by $(2)^{2^{1/6}}$) and fixed its value, leaving only six parameters to fit (we note that the $\langle R_{o(Br)} \rangle$ remained close to this value when allowed to float).

dx.doi.org/10.1021/ct3001969 | J. Chem. Theory Comput. 2012, 8, 2461–2473

The MP2 energies were best fitted with $n = 2.29$ for the $1/r^n$ term of V_{Elec} in eq 4, suggesting that the electrostatic component is not a classic Coulombic potential (where $n = 1$). To confirm this, we calculated the MP2 energies for BrU interacting with a formally neutral $H_2PO(OH)$ at three angles (100°, 140°, and 180°) and five distances (2.4 Å, 2.5 Å, 2.6 Å, 2.8 Å, and 3.4 Å) for each angle and compared them to the corresponding E_{Br} energies. We then subtracted the E_{Br} for the protonated neutral form from the anionic form of hypophosphite for each angle to determine the distance relationship for the effect of the charge on the X-bond energy. In this case, the average value for n was determined to be 2.4 ± 0.5. Thus, the value of $n \approx 2.5$ suggests that the electrostatic component falls between a charge−dipole ($n = 2$) and a dipole−dipole ($n = 3$) interaction, a reasonable description of the polarization effects that define, in this case, the distribution of charge across the surface of the bromine relative to the angle of approach by the acceptor atom. The value $\nu = 2.31$ orients the p_x and p_y orbitals ~12° from perpendicular, and the ratio of $A/B = 2.2$ defines an overall charge that is slightly positive (+0.14e) across the surface of the bromine (Figure 7), compared to the +0.047e from the MP2 calculations on BrU.

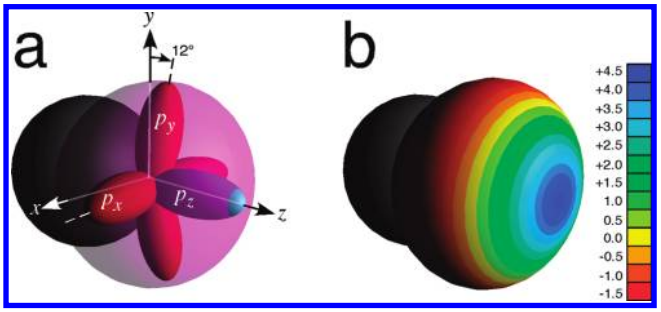

Figure 7. Atomic structure of Br2 as modeled by V_{LJ} (eq 1) and Z_{Br} (eq 2) functions applying the parameters in Table 1. (a) One bromine of a Br_2 molecule is shown with the outer p orbitals (fully occupied p_x and p_y orbitals in red, p_z empty orbital in blue) relative to their respective Cartesian reference axes. The polar flattening of the effective atomic radius along the z axis is associated with the depopulated p_z orbital. (b) Distribution of partial charge across the bromine surface, ranging from +5 to −2.0e.

Comparisons of QM and ffBXB Calculated to Experimental X-Bonding Energies. With the parameters in Table 1, the V_{Br} potentials could be combined with the standard AMBER potentials to define a complete force field for the bromine X-bond (the *ff*BXB), which can be applied to calculate the MM energies of the BrU···$H_2PO_2^-$ interactions at all geometries (Figure 6b−d). The resulting *ff*BXB energies fit the total MP2 calculated energies very well ($R = 0.96$). The QM and *ff*BXB approaches can be validated by comparing the calculated energies of interaction of BrU with the anionic hypophosphite or a dimethylphosphate (DMP^-) acceptors, the latter being a more complete model for the phosphodiester linkage between nucleotides, to the experimental X-bonding energies of the Br1J and Br2J conformations determined in the DNA junction system. Both the QM and *ff*BXB model calculations, when applied to the BrU···$H_2PO_2^-$ or BrU···DMP^- models in the Br1J or Br2J junction geometries, resulted in interaction energies that are well within the errors of the energies determined experimentally in the crystal system[7] and in solution[22] (Table 2). Thus, the resulting *ff*BXB functions replicate both the MP2 and experimental X-bonding energies of the DNA system used to derive the model.

Table 2. Comparison of Experimental and Calculated Enthalpies (kcal/mol) for Bromine X-Bonds in the Br1J and Br2J Conformations of DNA Junctions[7a]

	experimental ΔH_{X-H}		calculated energies ($H_2PO_2^-$/DMP^-)	
form	crystal assay[7]	calorimetric[22]	QM	*ff*BXB
Br1J	−2.0 ± 0.5		−1.44/−1.53	−1.97/−2.47
Br2J		−3.5 ± 1.3	−3.02/−3.06	−2.86/−4.63

[a]Interaction enthalpies for X minus H-bond (ΔH_{X-H}) determined from a crystallographic competition assay[7] and by differential scanning calorimetry in solution[22] are compared to X-bond energies from QM and *ff*BXB calculations applied to X-bonds of the BrU···$H_2PO_2^-$ or BrU···dimethylphosphate (DMP^-) model systems.

Potential Energy Landscapes for Bromine Interactions. The X-bond in the DNA junction is representative of those seen in other nucleic acid systems, including multistranded DNAs[33] and RNA,[34] with the bromine interacting with a single, formal negatively charged oxygen acceptor. For protein systems, this would also serve as an approximate model for halogen interactions with the charged oxygen acceptors of aspartate and glutamate side chains. It is useful, therefore, to derive a more general map for bromine interacting with a formally charged anionic acceptor. In this case, the *ff*BXB function shows the polar flattening associated with the V_{vdW} potential function (Figure 8a) and the anisotropic charge distribution of the V_{elec} potential function (Figure 8b).

The resulting total V_{Br} potential predicts a relatively deep potential energy well (−10.8 kcal/mol) at ~2.5 Å from the Br center and aligned along the σ-bond axis ($\Theta_1 = 180°$), as predicted (Figure 8c). The well for the isolated anionic oxygen is approximately 50% deeper and placed 0.15 Å shorter than that for the complete BrU···$H_2PO_4^-$ pair (at a depth of −7.6 kcal/mol and at ~2.7 Å from the bromine center) as calculated by the QM and *ff*BXB approaches. The differences can be attributed to noncovalent interactions between the additional atoms of the molecular system. A negative stabilizing potential is seen to extend to ≤130°, indicating that, although directional, Br X-bonds are stabilizing over a ≥90° range (±45° from linear). The zero point energy is at ~2.2 Å, while the stabilizing potential to −1 kcal/mol extends to >5 Å from the halogen center.

Formally charged oxygens represent only one type of X-bond acceptor seen in biological systems. The majority of biological X-bonds are to the carbonyl oxygens of the peptide bond in proteins,[3a,12c,14] although the oxygens of alcoholic and acidic side chains and sulfurs of methionine and cysteine residues can also serve as X-bond acceptors.[35] In addition, halogens are seen to be amphoteric, capable of serving as hydrogen bond acceptors. To determine how the *ff*BXB can be applied to other types of interactions, we compare the potential maps for charged oxygens (Figure 8c) to formally uncharged oxygens (partial charge −0.49e) and to a hydrogen (+0.5e) that can serve as an H-bond donor (Figure 9b). In each case, the calculations used the R_{vdW}, partial charge, and ε values for the acceptor atom, as defined by AMBER ff99.[19a]

The *ff*BXB potential map for a bromine to neutral oxygen interaction shows an energy minimum of −5.4 kcal/mol at 2.7 Å. The stabilization energy is approximately half of that for an

dx.doi.org/10.1021/ct3001969 | J. Chem. Theory Comput. 2012, 8, 2461−2473

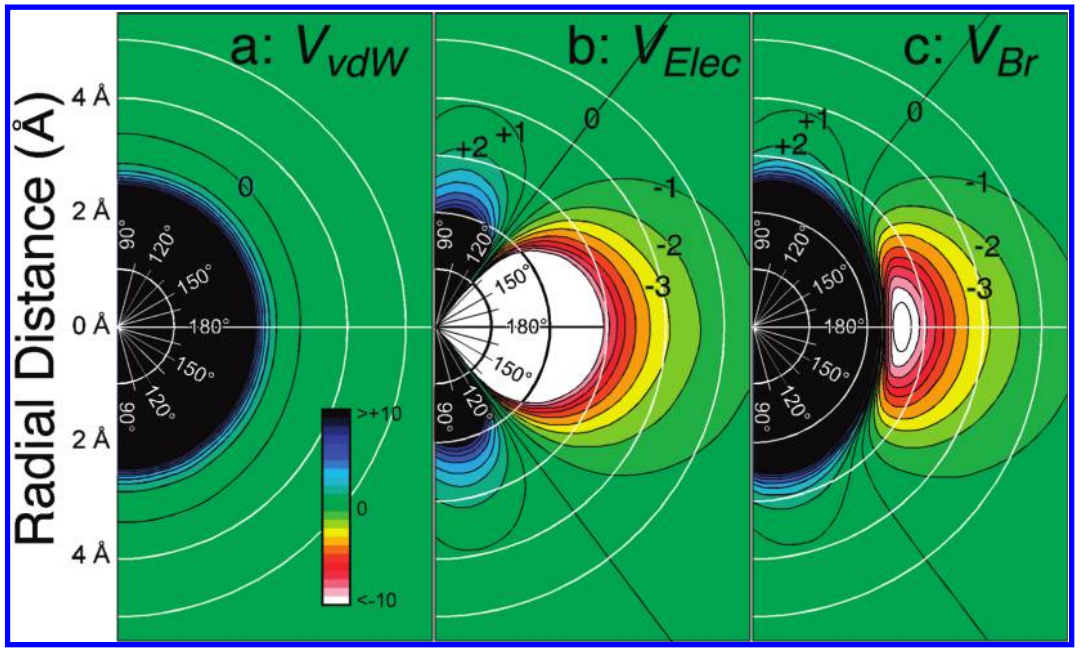

Figure 8. Potential energy maps calculated form the *ff*BXB of bromine interactions with formally charged oxygen. The V_{vdW} (a) from eq 1, V_{elec} (b) from eq 2, and total V_{Br} (c) from eq 6 are mapped onto polar plots, with concentric circles defining 1 Å radial distances from the bromine center and angles relative to the C−Br σ-bond labeled. The formally anionic O^- is assigned an effective partial charge of −0.85*e* to be consistent with the AMBER ff99 force field.

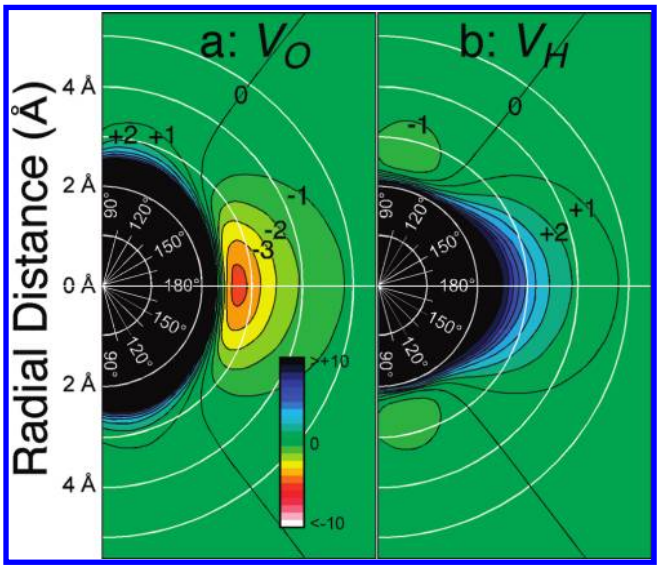

Figure 9. Energy landscapes calculated from the *ff*BXB functions for Br interactions with neutral oxygen (a) and hydrogen atoms (b). Energies are in kcal/mol. Although both the oxygen and hydrogen atoms are formally neutral, they were assigned partial charges of −0.49*e* and +0.5*e*, respectively, consistent with the AMBER ff99 force field.

anionic oxygen, consistent with the ∼2-fold difference in the AMBER assigned charge to the acceptor. Furthermore, the zero point distance is similar for both oxygens, while the optimum distance of interaction is only 5% longer for the neutral as opposed to the anionic X-bond acceptor and the −1 kcal/mol distance is contracted to <5 Å.

The *ff*BXB potential energy map for the Br···H interaction shows that the bromine can also serve as an H-bond acceptor in a direction approximately perpendicular to the X-bonding potential, as seen in crystal structures.[2b] The depth of the minimum energy well is calculated to be −1.7 kcal/mol at a distance of ∼2.5 Å from the bromine center and ∼11° from perpendicular as a result of most negative potential tipped slightly from Θ_1 of 90°. The electrostatic potential is sufficiently strong to pull the hydrogen to a distance ∼0.4 Å shorter than the sum of the R_{vdW} for the bromine and hydrogen; therefore, this interaction can be classified as a classic H-bond.

DISCUSSION

A set of potential energy functions is presented here that describe the aspherical shape and anisotropic distribution of electrostatic charge across the surface of a bromine substituent in molecular compounds. The functions very accurately reproduce the experimental and QM calculated geometry−energy relationships of various interactions with halogens, including X-bonds to charged, uncharged, and aromatic acceptors and H-bonds to electropositive donors. The hallmark of the *ff*BXB function is that it is derived from fundamental physicochemical properties of the halogen. The electrostatic function (V_{elec}) is clearly more akin to a dipole−dipole interaction in terms of the angular and distance dependence than to the standard Coulombic potential. This restricts both the range of angles and distances at which these interactions extend when compared to a true point charge electrostatic interaction.

Application to PEP Approach to Modeling Halogen Interactions. The alternative PEP approach to modeling X-bonding potentials is to add an extra positive charge with an R_{vdW} = 0 to mimic the electropositive crown resulting from polarization of the halogen. Previous studies that apply this model in a molecular mechanics approach have been successful in generally modeling interactions between X-bond donors and acceptors that correlate well with measures of affinity in protein−ligand complexes,[21] with distances between the interacting atoms within ∼0.3 Å of the corresponding distances observed in their crystal structures. We should note that the

Table 3. Parameters for PEP Approach to Model *ff*BXB Potential Energy Maps for Br···O^- Interactions, Based on the R_o and $\varepsilon_{B\rho}$ from the AMBER ff99 Force Field (PEP-a Model) and from the *ff*BXB Parameters (PEP-f Model)[a]

	steric parameters		electrostatic parameters			X-bond energies ($H_2PO_2^-$/DMP)	
model	R_o (Å)	ε_{Br} (kcal/mol)	Z_{Br} (e)	Z_ψ (e)	$r_{Br-\psi}$(Å)	Br1J	Br2J
PEP-a	2.22	0.32	−1.05 ± 0.26	+0.39 ± 0.04	1.856 ± 0.15	1.57/3.88	5.66/6.12
PEP-f	2.04	0.019	−0.17 ± 0.31	+0.54 ± 0.21	1.01 ± 0.13	−3.40/−4.96	−4.15/−5.99

[a]Interaction energies for X-bonds in the BrU···$H_2PO_2^-$ or BrU···dimethylphosphate (DMP^-) model systems, with a dielectric constant $D = 4r$, are compared between the two models.

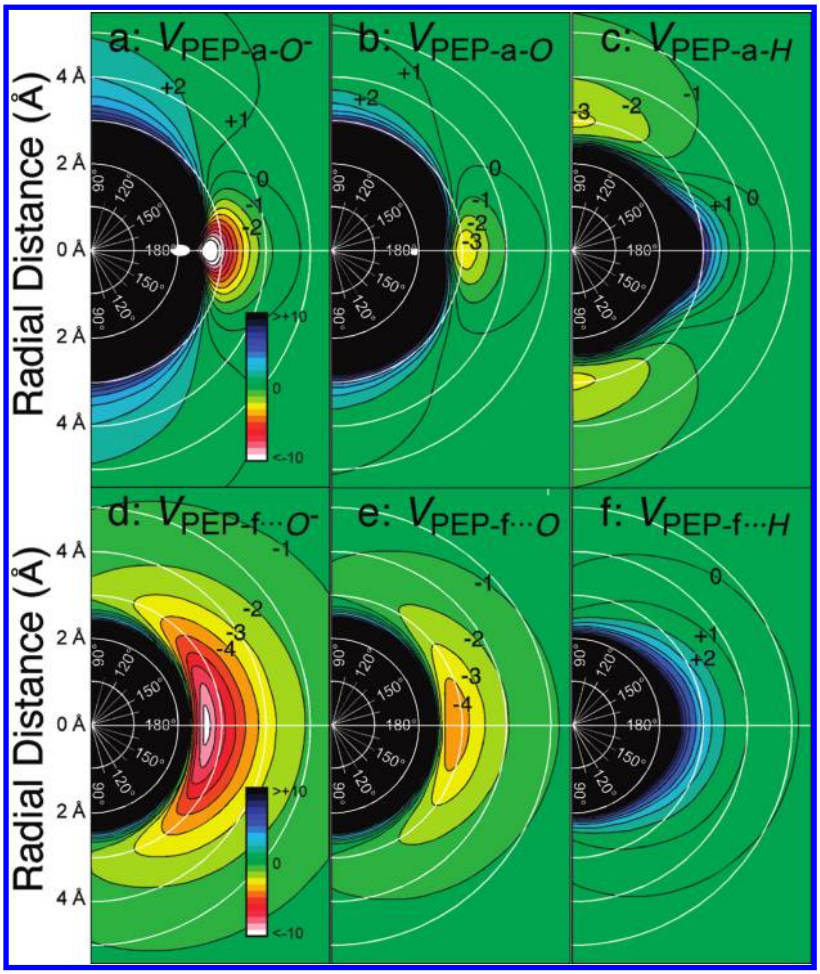

Figure 10. Potential energy landscape applying PEP models for the polarized bromine, applying the parameters from Table 3 to the AMBER ff99 force field. (a–c) Potential energy maps for bromine to anionic oxygen acceptor (Br···O^{1-}), bromine to neutral oxygen (Br···O), and bromine to neutral hydrogen (Br···H) interactions using the PEP-a model (using the standard R_o and ε_{Br} from the AMBER force field), with partial charges of −0.85 for the anionic oxygen, −0.49 for the formally neutral oxygen, and +0.5 for the neutral hydrogen as an H-bond donor. Energies are in kcal/mol. Concentric circles indicate the radial distances from the center of the bromine atom, with angles indicating the angle of approach of the acceptor atoms toward the C–Br bond. (d–f) The same as a–c, except using the PEP-f model with R_o and ε_{Br} from the *ff*BXB model.

PEP models derived here are very simplistic and primarily serve to compare and contrast this model to the *ff*BXB functions for the model systems in this particular study and should not be construed as being generally applicable to other systems (we leave the development of a more general model to those who are more invested in this approach).

To develop a PEP model, we define a partial negative charge (Z_{Br}) centered at the bromine atom and an added positive charge (Z_ψ) at some distance ($r_{Br-\psi}$) to model the σ-hole resulting from polarization of the halogen. Values for these three parameters were determined by fitting the energy-distance profile for the Br···O^{1-} interaction at $\Theta_1 = 180°$ (Figure 8c) using standard Coulombic (with a distance dependent dielectric $4r$, applying partial charges to nonhalogen atoms as they were in the *ff*BXB model) and van der Waals potentials. With the steric R_o and ε_{Br} parameters set to the standard values from AMBER ff99,[19a] the resulting parameters (PEP-a, Table 3) define the negative charge of the bromine to be overall 2.5-times that of the positive charge associated with the σ-hole, with the added charge at the standard r_{vdW} of the bromine (~1.85 Å from the Br center). The charges are thus those that best fit the QM energy profiles for this particular system.

The energy landscape calculated for the Br···O^{1-} pair (Figure 10a) is qualitatively very similar to that calculated using the *ff*BXB functions (Figure 8c) in terms of the depth of the

dx.doi.org/10.1021/ct3001969 | J. Chem. Theory Comput. 2012, 8, 2461–2473

energy well (−12 kcal/mol) at the optimum distance of interaction (∼2.7 Å). Thus, the PEP-a approach models the general features of the *ff*BXB energy landscape for the Br···O^{1-} interaction reasonable well (at Θ_1 = 180°, the PEP-a and *ff*BXB energies are correlated by an R = 0.932), although the energy well is deeper and narrower than that of the *ff*BXB model.

When applied to the Br1J and Br2J conformations of the BrU···$H_2PO_2^-$ or BrU···DMP$^-$ interacting pairs, however, the PEP-a model predicts positive energies of interaction for both conformations (Table 3), with the shorter Br2J being significantly more positive than Br1J. The energies of interaction for the reference anionic oxygens that are aligned nearly linearly with the C−Br bond are negative for both conformations, but the steric clash of the bromine with all the remaining atoms makes the overall energies positive. This suggests that the standard R_o and $\varepsilon_{B\rho}$ values in the AMBER force field as applied here do not properly model the van der Waals interactions of the bromine in this more complex system. To test this possibility, we redetermined a set of PEP parameters using the R_o and ε_{Br} values derived from the *ff*BXB approach (PEP-f), resulting in electrostatic terms that help to counterbalance the reduced steric interactions. These parameters correlate very well with the *ff*BXB energies at Θ_1 = 180° (E_{min} = −9.81 kcal/mol at 2.6 Å, R = 0.999 for the fit). Applying the PEP-f model to the Br1J and Br2J models with the $H_2PO_2^-$ and DMP$^-$ acceptors shows that the energies of interaction are negative for both conformations, with the shorter X-bond being more favorable than the longer interaction, as expected. Results from the PEP-f and *ff*BXB analyses suggest that the size of the halogen and energy terms for the van der Waals interaction need to be reduced relative to the standard AMBER definitions in order to properly describe the interactions in the experimental X-bonded DNA junction system.

A comparison of the overall landscape for the Br···O^{1-} interaction (Figure 10a and d) shows that although the depth and positions of the energy well for the two PEP models are similar, the well for the PEP-a model is very narrow (with the −1 kcal/mol contour extending from 180° to 150°) while the PEP-f well is very broad (having a negative energy completely encompassing the bromine atom). This same trend is seen for the interaction with the formally neutral oxygen (Br···O, Figure 10b and e). The extension of which can be attributed to the very small negative charge assigned to the bromine in the PEP-f model. The result is that for the Br···H interaction, the PEP-a model predicts energy wells of −3.5 kcal/mol at Θ_1= 90°, while no favorable interactions are predicted by the PEP-f model (Figure 10c and f). Thus, the PEP models derived here seem to trade accuracy in X-bonding behavior at $\Theta_1 \approx$ 180° in the PEP-f model for potential to form H-bonds at Θ_1= 90° in the PEP-a model. There probably exists a model between PEP-a and PEP-f that could account for both, but it is not clear how such a model can be derived using the current experimental system.

Comparison of ffBXB and PEP Models for Bromobenzene to Acetone Interactions. At this point, we can ask how the various models compare in their ability to model a bromine X-bond in a molecular system for which they were not initially optimized. Since most biological X-bonds are to the carbonyl oxygens of the peptide backbones in proteins, this comparison can be made to the energies of interaction (E_{Int}) for a bromobenzene to acetone model system from high-level MP2 calculations (Figure 11). These energies have been shown by Riley et al.[12b] to be tunable by varying the electron-withdrawing capability of the benzene ring by adding fluorines at various positions relative to the bromine.

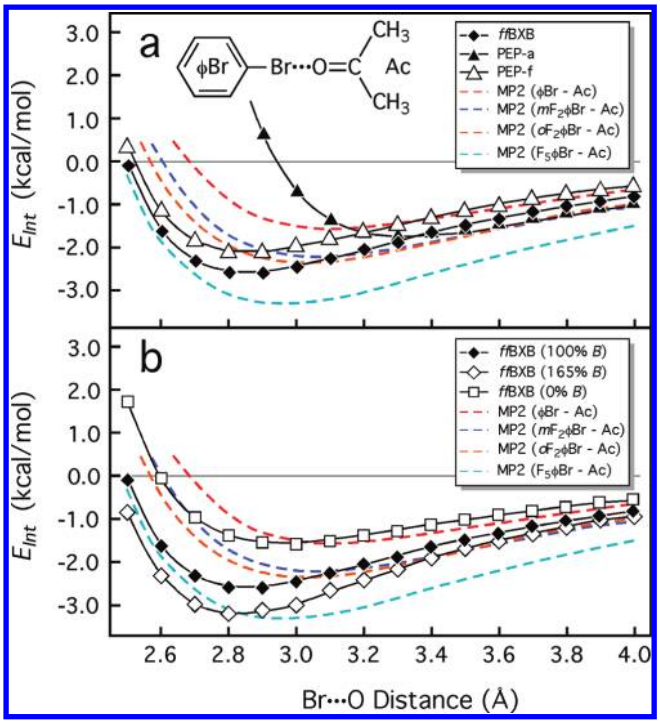

Figure 11. Comparison of energies for the interaction of acetone with bromobenzene and its fluorinated derivatives. (a) Comparison of MP2 to *ff*BXB and PEP-a and PEP-f models calculated energies of interaction (E_{Int}). Energies as a function of the carbonyl oxygen to bromine distance (at a 180° angle of approach) for the molecular interaction of acetone to bromobenzene (ϕBr, dashed red line), *meta*-difluorobromobenzene (*m*-$F_2\phi$Br, dashed blue line), *ortho*-difluorobromobenzene (*o*-$F_2\phi$Br, dashed orange line), and pentafluorobromobenzene ($F_5\phi$Br, dashed cyan line) are redrawn from Riley et al.[37] These energies are compared to those calculated from the *ff*BXB model (at 0.1 Å intervals in the O···Br distance) using the parameters from Table 1 (solid diamonds) and to the PEP-a (solid triangles) and PEP-f (solid diamonds) models. (b) Interaction energies from MP2 calculations compared to those from the *ff*BXB model with the electrostatic B term scaled by 100% (solid diamonds), 165% (open diamonds), or 0% (open squares).

If the quality of the two empirical models were judged solely on their abilities to reproduce the MP2 energies of the bromobenzene−acetone interaction, one would conclude that the PEP-a approach is better than either the *ff*BXB or PEP-f models (Table 4). The PEP-a calculated E_{Int} using the scaled partial charges from Table 3 (to yield an overall neutral donor molecule) is within 0.16 kcal/mol and positioned within 0.22 Å of the minimum of the MP2 energy curve—these deviations are similar to those obtained by Ibrahim for protein−ligand complexes. In contrast, although the E_{Int} from the *ff*BXB model falls well within the MP2 energy curves for bromobenzene and its various fluorinated derivatives, it does not exactly match any single MP2 curve. The depth of the energy well falls between those of the *o*-difluorobromobenzene and pentafluorobenzene energies (Table 4) at a distance ∼0.1 Å shorter than that for pentafluorobenzene. We must recognize, however, that the *ff*BXB and PEP-f parameters in Tables 2 and 3 were derived not for bromine attached to a benzene but for bromine to a uracil base, which is apparently much more electron-withdrawing than benzene. This is not surprising, as

Table 4. Interaction Energies Calculated for Acetone with Bromobenzene (ϕBr) and Its Fluorinated Variants as X-Bond Donors[a]

X-bond donor	E_{min} (kcal/mol)	R_{min} (Br···O)	Z_{Br}	$\sum\sigma$
ϕBr	−1.58	3.10 Å	−0.0412e	0.0
m-F_2-ϕBr	−2.22	3.05 Å	0.0012e	0.68
o-F_2-ϕBr	−2.37	3.00 Å	0.0255e	(0.93)
F_5-ϕBr	−3.34	2.96 Å	0.0675e	(1.67)
ϕBr (*ff*BXB, 100% *B*)	−2.75	2.85 Å		[1.36]
ϕBr (*ff*BXB, 0% *B*)	−1.58	2.97 Å		[0.137]
ϕBr (*ff*BXB, 165% *B*)	−3.34	2.80 Å		[1.98]
ϕBr (PEP-a)	−1.74	3.32 Å		[0.31]
ϕBr (PEP-f)	−1.74	3.32 Å		[0.31]
m-F_2-p-F-ϕBr			0.0043e	0.74
Br-Uracil			0.0470e	(1.44)
o-F_2-m-F_2-ϕBr			0.0450e	(1.40)

[a]The minimum energies of interaction (E_{min}) and the Br···O distances for the E_{min} (R_{min}) for acetone interacting with ϕBr, *m*-difluoro-ϕBr (*m*-F_2-ϕBr), *o*-difluoro-ϕBr (*o*-F_2-ϕBr), and pentafluor-ϕBr (F_5-ϕBr) from Riley et al. are compared to those calculated with the *ff*BXB and the PEP methods. In addition, the overall partial charges of the bromines (Z_{Br}) in each of the fluorinated variants were estimated from MP2, *ff*BXB, or PEP approaches. Finally, the substituent effects of each donor compound (as reflected in the summed Hammett σ constants for the fluorine substituents ($\sum\sigma$)) are compared, applying reported values for the *meta* and *para* positions,[39] estimated for the *ortho* position from the Z_{Br} values (in parentheses), or from E_{min} values (in brackets), see text for description.

bromine attached to a heterocyclic ring (as in bromopyrimidine, a model that is more analogous to uracil) has been shown to form a stronger X-bond to acetone than bromobenzene.[36] By comparing the *ff*BXB energy to those of the various fluorinated X-bond donors, we can estimate that the uracil base is equivalent in electron-withdrawing potential as a tetrafluorinated benzene.

To quantify the effective electron withdrawing ability of the uracil base in our initial model system, we first calculated the effective charge of the bromine (Z_{Br}) in bromobenzene, in 3,5-difluorobromobenzene, and in 3,4,5-trifluorobromobenzene and related these values to the standard Hammett σ coefficient[38] as the measure of the inductive effects for fluorine substituents at the *meta* and *para* positions. As expected, increasing the electron-withdrawing property of the benzene ring with added fluorines exaggerated the polarization and, consequently, the effective overall positive charge of the bromine atom (Table 4). The resulting linear relationship $\sum\sigma = 16.5Z_{Br} + 0.684$ ($R^2 = 0.999$, where $\sum\sigma$ is the sum of the σ constants) allowed us to estimate a $\sigma = 0.46$ for an *ortho*-fluorine substituent. The inductive effects are linearly related to the energies of interaction of the fluorinated variants of bromobenzene with acetone according to the equation $\sum\sigma = -1.05E_{Int} - 1.52$ ($R^2 = 0.985$). By comparison, the Z_{Br} from MP2 calculations on BrU estimates $\sum\sigma = 1.44$, while the E_{Int} calculated for the bromobenzene−acetone pair from the *ff*BXB parameters is equivalent to an effective $\sum\sigma = 1.36$. The uracil base, therefore, apparently has an equivalent electron-withdrawing capacity as a tetrafluorinated benzene and is accurately modeled by the *ff*BXB parameters.

The *ff*BXB and energies can be readily tuned to that of the pentafluorobenzene by scaling the electrostatic *B* term of the model by 165% and to that of the unfluorinated bromobenzene by scaling this term to 0 (Figure 11b). With $B = 0$, we see that the *ff*BXB model fares very well in comparison with the PEP-a approach, with a Br···O distance for the E_{Int} optimum that is 0.13 Å shorter than the MP2 curve. The E_{Int} for each of the scaled *B* terms can be linearly related to the magnitude of the electron-withdrawing capacity of each of the corresponding fluorinated derivatives by $B = 1.38\sum\sigma - 0.173$ ($R = 0.9995$). The effect of substitutents around the benzene ring on the polarizability of the bromine can, therefore, be readily modeled through a standard measure of the electron withdrawing ability of the molecule to which the halogen is attached. An analogous analysis allows the Z_ψ term of the PEP-f model to be scaled relative to the $\sum\sigma$ parameters according to the relationship $Z_\psi = 0.156\sum\sigma + 0.385$ ($R = 0.9997$), resulting in curves similar to those of the *ff*BXB relationships.

The *ff*BXB optimum energies consistently fall at distances 0.13 to 0.16 Å shorter than of those from MP2 calculations. One can argue that the reduced polarizability of the bromine in the bromobenzene model should result in a slightly larger van der Waals radius for the halogen, particularly in the direction of the σ hole. In this case, increasing $\langle R_{vdW(Br)} \rangle$ by 0.1 Å would place all of the energy minima to within 0.05 Å of the MP2 calculated curves for the bromobenzene···acetone pair.

CONCLUSIONS

The *ff*BXB model now provides a complete description of the geometric constraints that allow us to explore the great potential of X-bonds as well as H-bonds as molecular tools for the design and synthesis of new halogenated therapeutic agents and biomolecular materials. The resulting set of potential energy functions very accurately models the structure−energy relationships for bromine to anionic oxygen X-bonds calculated from QM analyses and observed experimentally in a DNA junction biomolecular system and can be extended to predict the X-bonding and perpendicular H-bonding potential of halogens. The *ff*BXB functions can be directly incorporated into current molecular mechanics force fields, in much the same manner that angular dependent H-bonds have been incorporated,[10] or they can be used to derive parameters for a more conventional PEP approach to simulating the polarization effects of halogens.

Both the *ff*BXB and PEP approaches can, to varying degrees, be applied to simulate bromine halogen interactions in biomolecules other than the DNA system used in the current study, including X-bonds to other types of acceptors and H-bonds. The simulations of X-bonding to the carbonyl oxygen of acetone mimics the energies and geometries observed in protein−ligand systems and, therefore, demonstrate the utility of such empirical force fields for inhibitor design. In this case, we show that the electrostatic potentials for the interactions can be tuned by considering the electron withdrawing potential of the molecule that is halogenated. We can, thus, propose that in designing a new halogenated version of a lead inhibitor, the electrostatic parameters can be initially defined according to standard measures of this property, which would result in much more accurate energies of interactions and, consequently, more accurate dissociation constants specific for that particular system. In the *ff*BXB model, this is achieved by a simple and straightforward scaling of the electrostatic *B* term. For the PEP approach, however, it is clear that the standard descriptors of the size of the bromine as currently implemented in, for

example, the AMBER force field may not properly model the effects on the associated steric and dispersive forces.

Obviously, these potential energy functions do not explicitly treat either entropy or solvent effects on the energies of molecular halogen interactions. For example, bromines are known to be hydrophobic substituents, which may initially appear to be contradictory to the strong electrostatic contributions to the H- and X-bonding interactions the halogen is expected to make with water; however, both these interactions are predicted by the energy functions to be highly directional, which would limit the configurational space available and, thus, the entropy of each interacting water molecule. According to the Lum et al. model,[40] this reduced solvent entropy would contribute to the hydrophobicity of halogen substituents. Once incorporated into current force fields commonly used for molecular simulations and molecular docking, we expect that both conformational and solvent entropy effects can be modeled using established free-energy methods,[1] thereby providing a test for this hypothesis.

Finally, although the *ff*BXB functions were derived specifically for bromine in the current study, the results provide a strategy to parametrize the functions for all other halogens (chlorine and iodine in particular) and, potentially, for other group V and VI atoms that show significant σ-hole polarization.[9,41]

AUTHOR INFORMATION

Corresponding Author

*Phone: 1-970-491-0569. Fax: 1-970-491-0494. E-mail: Shing.Ho@colostate.edu.

Notes

The authors declare no competing financial interest.

ACKNOWLEDGMENTS

This work was supported in part by funds from Colorado State University and a grant from the National Science Foundation (CHE-1152494).

REFERENCES

(1) (a) Steinbrecher, T.; Labahn, A. Towards Accurate Free Energy Calculations in Ligand Protein-Binding Studies. *Curr. Med. Chem.* **17**, 767−785. (b) Huang, N.; Jacobson, M. P. Physics-based methods for studying protein-ligand interactions. *Curr. Opin. Drug Discovery Dev.* **2007**, *10*, 325−331. (c) Boyce, S. E.; Mobley, D. L.; Rocklin, G. J.; Graves, A. P.; Dill, K. A.; Shoichet, B. K. Predicting ligand binding affinity with alchemical free energy methods in a polar model binding site. *J. Mol. Biol.* **2009**, *394*, 747−763.

(2) (a) Politzer, P.; Murray, J. S.; Lane, P. Sigma-hole bonding and hydrogen bonding: Competitive interactions. *Int. J. Quantum Chem.* **2007**, *107*, 3046−3052. (b) Lu, Y.; Wang, Y.; Xu, Z.; Yan, X.; Luo, X.; Jiang, H.; Zhu, W. C-X···H contacts in biomolecular systems: how they contribute to protein-ligand binding affinity. *J. Phys. Chem. B* **2009**, *113*, 12615−12621.

(3) (a) Auffinger, P.; Hays, F. A.; Westhof, E.; Ho, P. S. Halogen bonds in biological molecules. *Proc. Natl. Acad. Sci. U. S. A.* **2004**, *101*, 16789−16794. (b) Metrangolo, P.; Neukirch, H.; Pilati, T.; Resnati, G. Halogen bonding based recognition processes: A world parallel to hydrogen bonding. *Acc. Chem. Res.* **2005**, *38*, 386−395.

(4) Hassel, O. Structural aspects of interatomic charge-transfer bonding. In *Nobel Lectures, Chemistry 1963−1970*; Elsevier Publishing Company: Amsterdam, 1972.

(5) Metrangolo, P.; Resnati, G. Chemistry: Halogen versus hydrogen. *Science* **2008**, *321*, 918−919.

(6) (a) Matter, H.; Nazare, M.; Gussregen, S.; Will, D. W.; Schreuder, H.; Bauer, A.; Urmann, M.; Ritter, K.; Wagner, M.; Wehner, V. Evidence for C-Cl/C-Br...pi interactions as an important contribution to protein-ligand binding affinity. *Angew. Chem., Int. Ed. Engl.* **2009**, *48*, 2911−2916. (b) Lam, P. Y. S.; Clark, C. G.; Smallwood, A. M.; Alexander, R. S. Structure-based drug design utilizing halogen bonding: Factor Xa inhibitors. In *The 238th ACS National Meeting*; Metrangolo, P., Resnati, G., Eds.; American Chemical Society: Washington, DC, 2009; Vol. ORGN, p 58. (c) Xu, Z.; Liu, Z.; Chen, T.; Wang, Z.; Tian, G.; Shi, J.; Wang, X.; Lu, Y.; Yan, X.; Wang, G.; Jiang, H.; Chen, K.; Wang, S.; Xu, Y.; Shen, J.; Zhu, W. Utilization of halogen bond in lead optimization: a case study of rational design of potent phosphodiesterase type 5 (PDE5) inhibitors. *J. Med. Chem.* **2011**, *54*, 5607−5611.

(7) Voth, A. R.; Hays, F. A.; Ho, P. S. Directing macromolecular conformation by halogen bonds. *Proc. Natl. Acad. Sci. U. S. A.* **2007**, *104*, 6188−6193.

(8) Ouvrard, C.; Le Questel, J. Y.; Berthelot, M.; Laurence, C. Halogen-bond geometry: a crystallographic data-base investigation of dihalogen complexes. *Acta Crystallogr.* **2003**, *B59*, 512−526.

(9) Murray, J. S.; Lane, P.; Clark, T.; Politzer, P. Sigma-hole bonding: molecules containing group VI atoms. *J. Mol. Model.* **2007**, *13* (10), 1033−1038.

(10) Lii, J. H.; Allinger, N. L. The Important Role of Lone-Pairs in Force Field (MM4) Calculations on Hydrogen Bonding in Alcohols. *J. Phys. Chem. A* **2008**, *112*, 11903−11913.

(11) Lommerse, J. P. M.; Stone, A. J.; Taylor, R.; Allen, F. H. The nature and geometry of intramolecular interactions between halogens and oxygen or nitrogen. *J. Am. Chem. Soc.* **1996**, *118*, 3108−3116.

(12) (a) Voth, A. R.; Ho, P. S. The Role of Halogen Bonding in Inhibitor Recognition and Binding by Protein Kinases. *Curr. Topics Med. Chem.* **2007**, *7*, 1336−1348. (b) Riley, K. E.; Murray, J. S.; Fanfrlik, J.; Rezac, J.; Sola, R. J.; Concha, M. C.; Ramos, F. M.; Politzer, P. Halogen bond tunability I: the effects of aromatic fluorine substitution on the strengths of halogen-bonding interactions involving chlorine, bromine, and iodine. *J. Mol. Model.* **2011**, *17*, 3309−18. (c) Parisini, E.; Metrangolo, P.; Pilati, T.; Resnati, G.; Terraneo, G. Halogen bonding in halocarbon-protein complexes: a structural survey. *Chem. Soc. Rev.* **2011**, *40*, 2267−78.

(13) Lu, Y.; Shi, T.; Wang, Y.; Yang, H.; Yan, X.; Luo, X.; Jiang, H.; Zhu, W. Halogen bonding--a novel interaction for rational drug design? *J. Med. Chem.* **2009**, *52*, 2854−62.

(14) Voth, A. R.; Khuu, P.; Oishi, K.; Ho, P. S. Halogen bonds as orthogonal molecular interactions to hydrogen bonds. *Nat. Chem.* **2009**, *1*, 74−79.

(15) Politzer, P.; Murray, J. S.; Concha, M. C. Halogen bonding and the design of new materials: organic bromides, chlorides and perhaps even fluorides as donors. *J. Mol. Model.* **2007**, *13*, 643−650.

(16) Ibrahim, M. A. A. Performance Assessment of Semiempirical Molecular Orbital Methods in Describing Halogen Bonding: Quantum Mechanical and Quantum Mechanical/Molecular Mechanical-Molecular Dynamics Study. *J. Chem. Inf. Model.* **2011**, *51*, 2549−2559.

(17) Dobes, P.; Rezac, J.; Fanfrlik, J.; Otyepka, M.; Hobza, P. Semiempirical quantum mechanical method PM6-DH2X describes the geometry and energetics of CK2-inhibitor complexes involving halogen bonds well, while the empirical potential fails. *J. Phys. Chem. B* **2011**, *115*, 8581−9.

(18) Muzet, N.; Guillot, B.; Jelsch, C.; Howard, E.; Lecomte, C. Electrostatic complementarity in an aldose reductase complex from ultra-high-resolution crystallography and first-principles calculations. *Proc. Natl. Acad. Sci. U. S. A.* **2003**, *100*, 8742−7.

(19) (a) Case, D. A.; Cheatham, T. E.; Darden, T.; Gohlke, H.; Luo, R.; Merz, K. M., Jr.; Onufriev, A.; Simmerling, C.; Wang, B.; Woods, R. J. The Amber biomolecular simulation programs. *J. Comput. Chem.* **2005**, *26*, 1668−88. (b) Vreven, T.; Morokuma, K.; Farkas, O.; Schlegel, H. B.; Frisch, M. J. Geometry optimization with QM/MM, ONIOM, and other combined methods. I. Microiterations and constraints. *J. Comput. Chem.* **2003**, *24*, 760−769.

(20) Ibrahim, M. A. AMBER empirical potential describes the geometry and energy of noncovalent halogen interactions better than

advanced semiempirical quantum mechanical method PM6-DH2X. *J. Phys. Chem. B* **2012**, *116*, 3659−69.
(21) (a) Sponer, J.; Riley, K. E.; Hobza, P. Nature and magnitude of aromatic stacking of nucleic acid bases. *Phys. Chem. Chem. Phys.* **2008**, *10*, 2595−610. (b) Ibrahim, M. A. A. Molecular Mechanical Study of Halogen Bonding in Drug Discovery. *J. Comput. Chem.* **2011**, *32*, 2564−2574.
(22) Gribble, G. W. The diversity of naturally produced organohalogens. *Chemosphere* **2003**, *52*, 289−297.
(23) Peebles, S. A.; Fowler, P. W.; Legon, A. C. Anisotropic repulsion in complexes B···C12 and B···HCI: the shape of the chlorine atom-in-a-molecule. *Chem. Phys. Lett.* **1995**, *240*, 130−134.
(24) Møller, C.; Plesset, M. S. Note on an Approximation Treatment for Many-Electron Systems. *Phys. Rev.* **1934**, *46*, 618−622.
(25) Bondi, A. van der Waals volumes and radii. *J. Phys. Chem.* **1964**, *68*, 441−451.
(26) Nyburg, S. Polar flattening: Non-spherical effective shapes of atoms in crystals. *Acta Crystallogr.* **1979**, *A35*, 641−645.
(27) Armstrong, J. *General, Organic, and Biochemistry: An Applied Approach*; Brooks/Cole: Belmont, CA, 2012.
(28) Wang, J.; Wolf, R. M.; Caldwell, J. W.; Kollman, P. A.; Case, D. A. Development and testing of a general amber force field. *J. Comput. Chem.* **2004**, *25*, 1157−1174.
(29) Brooks, B. R.; Brooks, C. L.; Mackerell, A. D., Jr.; Nilsson, L.; Petrella, R. J.; Roux, B.; Won, Y.; Archontis, G.; Bartels, C.; Boresch, S.; Caflisch, A.; Caves, L.; Cui, Q.; Dinner, A. R.; Feig, M.; Fischer, S.; Gao, J.; Hodoscek, M.; Im, W.; Kuczera, K.; Lazaridis, T.; Ma, J.; Ovchinnikov, V.; Paci, E.; Pastor, R. W.; Post, C. B.; Pu, J. Z.; Schaefer, M.; Tidor, B.; Venable, R. M.; Woodcock, H. L.; Wu, X.; Yang, W.; York, D. M.; Karplus, M. CHARMM: the biomolecular simulation program. *J. Comput. Chem.* **2009**, *30*, 1545−1614.
(30) Van Der Spoel, D.; Lindahl, E.; Hess, B.; Groenhof, G.; Mark, A. E.; Berendsen, H. J. GROMACS: fast, flexible, and free. *J. Comput. Chem.* **2005**, *26*, 1701−18.
(31) Paizs, B.; Suhai, S. Comparative study of BSSE correction methods at DFT and MP2 levels of theory. *J. Comput. Chem.* **1998**, *19*, 575−584.
(32) Ferrara, P.; Gohlke, H.; Price, D. J.; Klebe, G.; Brooks, C. L. Assessing scoring functions for protein-ligand interactions. *J. Med. Chem.* **2004**, *47*, 3032−3047.
(33) (a) Sunami, T.; Kondo, J.; Hirao, I.; Watanabe, K.; Miura, K.; Takenaka, A. Structures of d(GCGAAGC) and d(GCGAAAGC) (tetragonal form): a switching of partners of the sheared G.A pairs to form a functional G.AxA.G crossing. *Acta Crystallogr., Sect. D: Biol. Crystallogr.* **2004**, *60* (Pt 3), 422−431. (b) Sunami, T.; Kondo, J.; Hirao, I.; Watanabe, K.; Miura, K. I.; Takenaka, A. Structure of d(GCGAAAGC) (hexagonal form): a base-intercalated duplex as a stable structure. *Acta Crystallogr., Sect. D: Biol. Crystallogr.* **2004**, *60* (Pt 1), 90−96.
(34) Gilbert, S. D.; Reyes, F. E.; Edwards, A. L.; Batey, R. T. Adaptive ligand binding by the purine riboswitch in the recognition of guanine and adenine analogs. *Structure* **2009**, *17*, 857−868.
(35) (a) Liu, L.; Baase, W. A.; Matthews, B. W. Halogenated benzenes bound within a non-polar cavity in T4 lysozyme provide examples of I...S and I...Se halogen-bonding. *J. Mol. Biol.* **2009**, *385*, 595−605. (b) Vallejos, M.; Auffinger, P.; Ho, P.; Himmel, D. M. Halogen interactions in biomolecular crystal structures. *International Tables for Crystallography*; International Union of Crystallography: Chester, England, 2010*F*
(36) Riley, K. E.; Murray, J. S.; Politzer, P.; Concha, M. C.; Hobza, P. Br···O Complexes as probes of factors affecting halogen bonding: Interactions of bromobenzenes and bromopyrimidines with acetone. *J. Chem. Theory Comput.* **2009**, *5*, 155−163.
(37) Egner, U.; Kratzschmar, J.; Kreft, B.; Pohlenz, H. D.; Schneider, M. The target discovery process. *ChemBioChem* **2005**, *6*, 468−479.
(38) Hammett, L. P. The Effect of Structure upon the Reactions of Organic Compounds. Benzene Derivatives. *J. Am. Chem. Soc.* **1937**, *59*, 96−103.
(39) McDaniel, D. H.; Brown, H. C. An Extended Table of Hammett Substituent Constants Based on the Ionization of Substituted Benzoic Acids. *J. Org. Chem.* **1958**, *23*, 420−427.
(40) Lum, K.; Chandler, D.; Weeks, J. D. Hydrophobicity at Small and Large Length Scales. *J. Phys. Chem. B* **1999**, *103*, 4570−4577.
(41) Clark, T.; Hennemann, M.; Murray, J. S.; Politzer, P. Halogen bonding: the sigma-hole. Proceedings of "Modeling interactions in biomolecules II", Prague, September 5th-9th, 2005. *J. Mol. Model.* **2007**, *13*, 291−296.